Oregon State University
College of Engineering

ASME
IMECE® 2024

International Mechanical Engineering
Congress & Exposition®

Additive Manufacturing of Lattice Structures for Catalyst Applications

Nahal Ghanadi, Kwangtae Son, Brian Paul, Somayeh Pasebani
Oregon state University

ASME IMECE® 2024
International Mechanical Engineering Congress & Exposition®

Oregon State University College of Engineering

Introduction

- **Additive Manufacturing (AM) Revolution**
  - Enables complex geometries and customized components
  - Applications in aerospace, automotive, biomedical, and energy sectors
- **Laser Powder Bed Fusion (LPBF)**
  - High precision in fabricating intricate designs
  - Layer-by-layer fusion using a high-energy laser
- **Advantages of Lattice Architectures**
  - Weight reduction
  - Mechanical performance optimization
  - Enhanced functionality (thermal management, catalytic activity)
- **Applications**
  - Aerospace and automotive: Improved fuel efficiency
  - Biomedical implants: Mimic bone properties, promote osseointegration
  - Heat exchangers and fluid systems: Enhanced heat transfer, optimized fluid distribution

2Create Metal 3D Printer (LPBF)

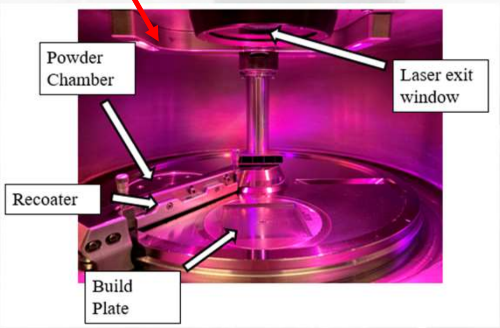

Lattices in Microchannel Technology

Foams integrated within reactors enhance catalytic reactions, increasing exposure and efficiency.

- **Catalyst Innovation:**
  - New catalyst efficiently produces butene-rich olefins from ethanol.
  - Reduces alcohol-to-jet (ATJ) processing steps by eliminating one-unit operation.
- **Microchannel Technology:**
  - Leverages microchannel technology for energy savings and process intensification.
  - Compact modular reactors enhance efficiency.
- **Additive Manufacturing Impact:**
  - Adoption of state-of-the-art additive manufacturing methods.
  - Potential for significant reduction in manufacturing costs.

Reactor catalyst volume (4 pies)

Challenges and Objectives

- **Geometrical Complexity**
  - Strut thickness, pore size, and surface roughness are critical
- **Need for Specific Investigation**
  - Solid structures' parameters may not yield desired lattice outcomes
  - Limited understanding of LPBF parameters on lattice structures
- **Primary Goal**
  - Investigate the impact of LPBF processing parameters on lattice structures
- **Focus Areas**
  - Geometrical accuracy
  - Surface morphology
  - Mechanical properties

Inconel 718 Overview

- **Material Selection**
  - Nickel-based superalloy
  - Exceptional mechanical properties
  - Corrosion resistance and high-temperature performance
- **Suitability for LPBF**
  - High strength-to-weight ratio
  - Ideal for complex, lightweight lattice geometries

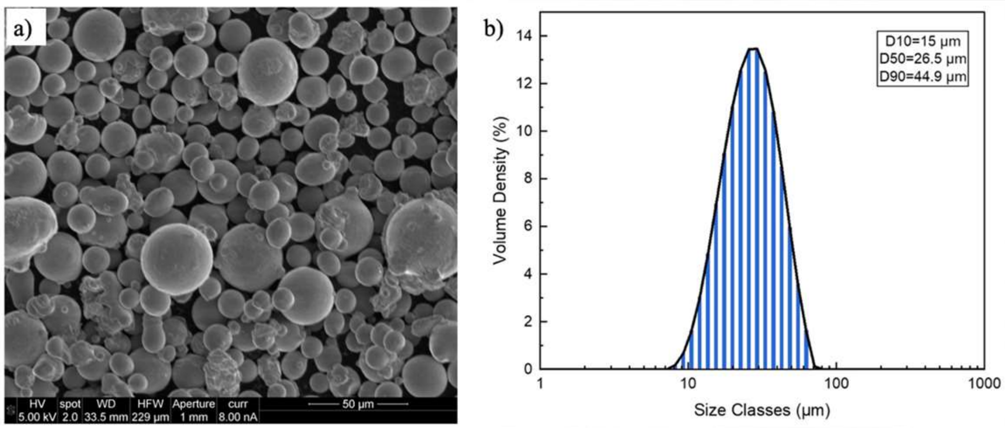

Inconel 718 powder characteristics (a) surface morphology of the powder, (b) PSD analysis plot

The chemical compositions of the Inconel 718 powder (wt%).

Element	Ni	Cr	Fe	Nb+Ta	Mo	Co	Ti
Weight, %	54.22	18.5	17.46	4.86	3.09	0.2	1.03

Oregon State University
College of Engineering

Dode-medium Lattice Design

- **Lattice Structure**
  - Target porosity: 80%
  - Unit cell size: 2 mm
  - Open Pore size: 1.13 mm
  - Strut thickness: 0.26 mm
  - Struts at 45° to the build direction

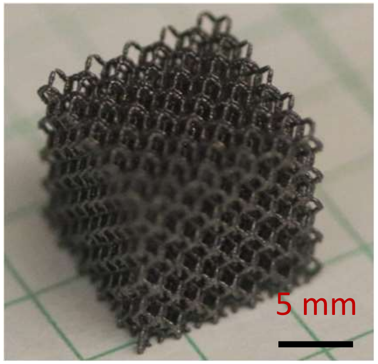

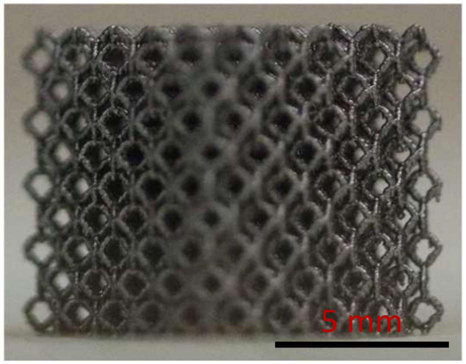

An example of the fabricated Dode-medium lattice structures

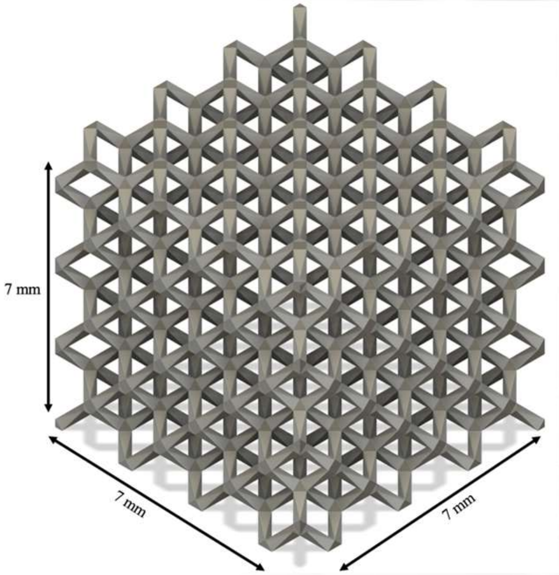

Original schematics of the Dode-medium lattice design [1,2,3]

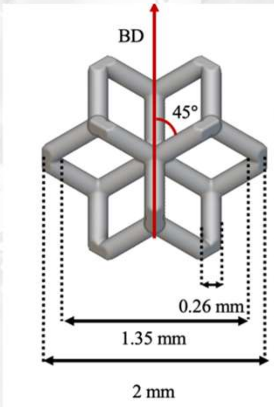

Dode-medium unit cell

1. Hazeli, K.; Babamiri, B. B.; Indeck, J.; Minor, A.; Askari, H. Microstructure-Topology Relationship Effects on the Quasi-Static and Dynamic Behavior of Additively Manufactured Lattice Structures. *Mater Des* **2019**, *176*, 107826.
2. Bahrami Babamiri, B.; Askari, H.; Hazeli, K. Deformation Mechanisms and Post-Yielding Behavior of Additively Manufactured Lattice Structures. *Mater Des* **2020**, *188*, 108443.
3. Hazeli, K.; June, D.; Anantwar, P.; Babamiri, B. B. Mechanical Behavior of Additively Manufactured GRCop-84 Copper Alloy Lattice Structures. *Addit Manuf* **2022**, *56*, 102928. https://doi.org/10.1016/j.addma.2022.102928.

Top Surface Morphology

- Solid Blocks
  - Low laser power/high scanning speed: Rough surfaces, visible pores, LOF defects
  - High energy input: Signs of keyhole mode melting, scanning tracks visible

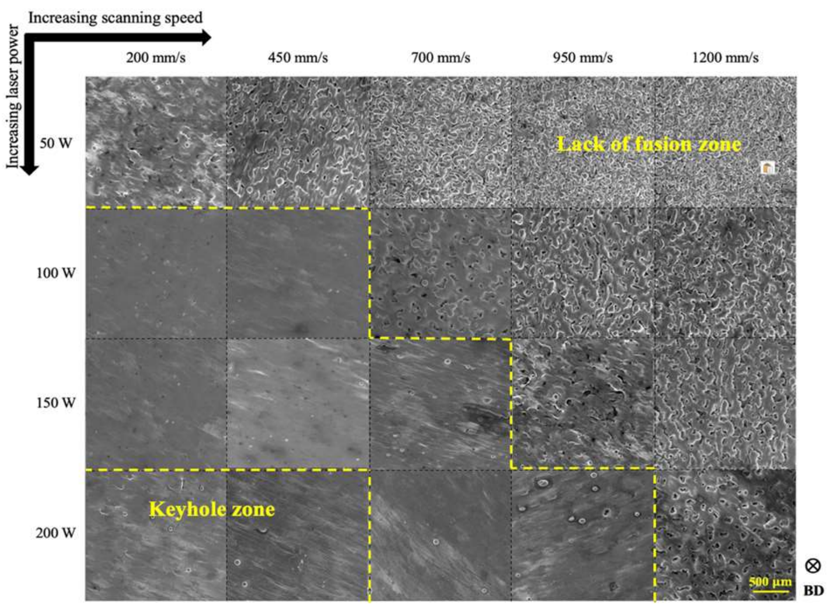

Top surface SEM micrograph of the Inc 718 solid blocks fabricated with different processing parameters.

- Lattice Structures
  - Low energy input: Larger open pore sizes, thinner struts
  - High energy input: Smaller pores, thicker struts, potential overgrowth

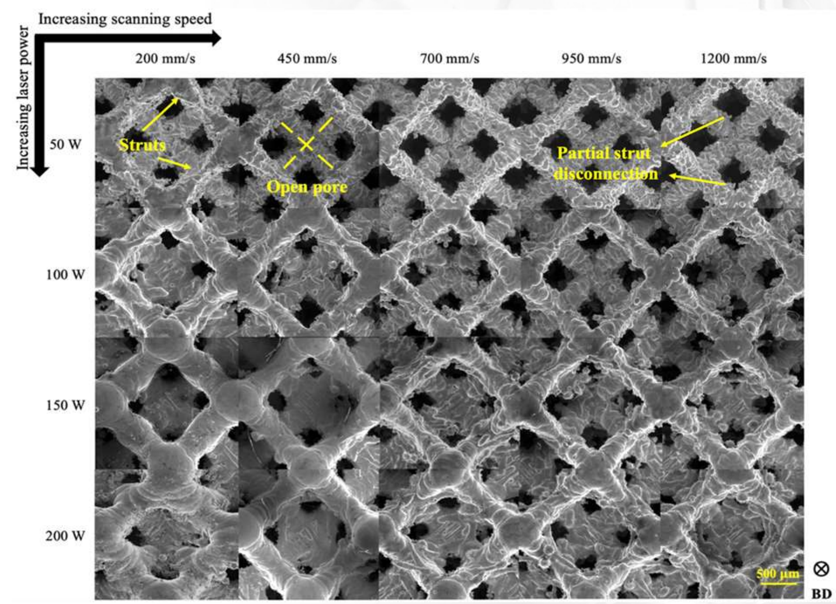

Top surface SEM micrograph of of the Inc 718 lattices fabricated with different processing parameters.

ASME IMECE® 2024 International Mechanical Engineering Congress & Exposition®

Oregon State University College of Engineering

Side Surface Morphology

- Side surfaces generally rougher than top surfaces
- Lattices exhibit more pronounced differences due to geometry
- Layer-by-layer deposition
- Partially adhered powder particles

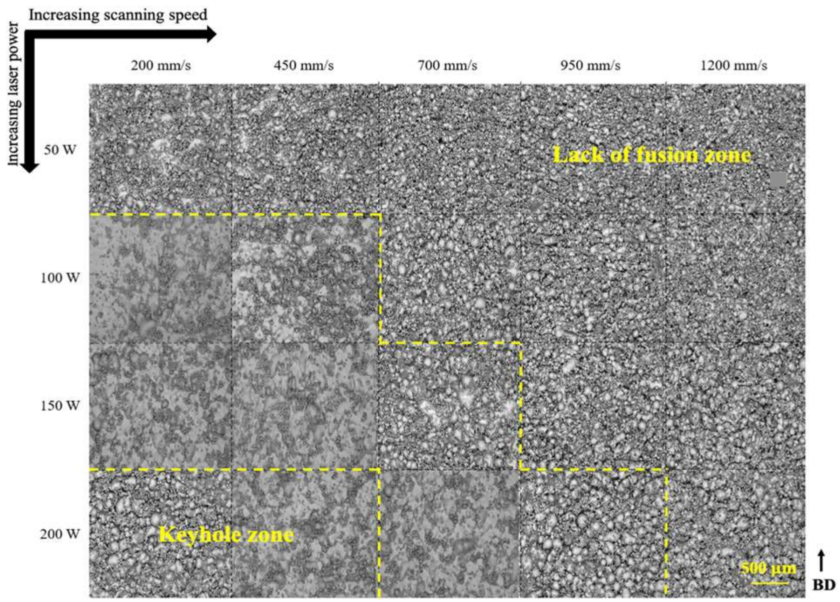

Side surface SEM micrographs of the Inconel 718 solid blocks blocks fabricated with different processing parameters.

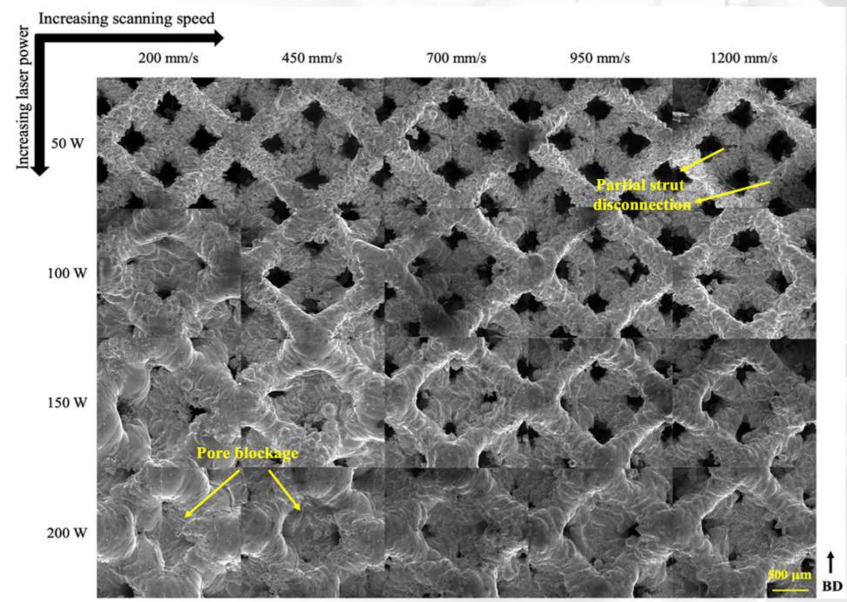

Side surface SEM micrographs of the Inconel 718 Lattice structures blocks fabricated with different processing parameters.

Relative Density and open cell Porosity Maps

- **Solid Blocks**
  - Relative density varies with processing parameters
  - Density (~99%) at optimal settings

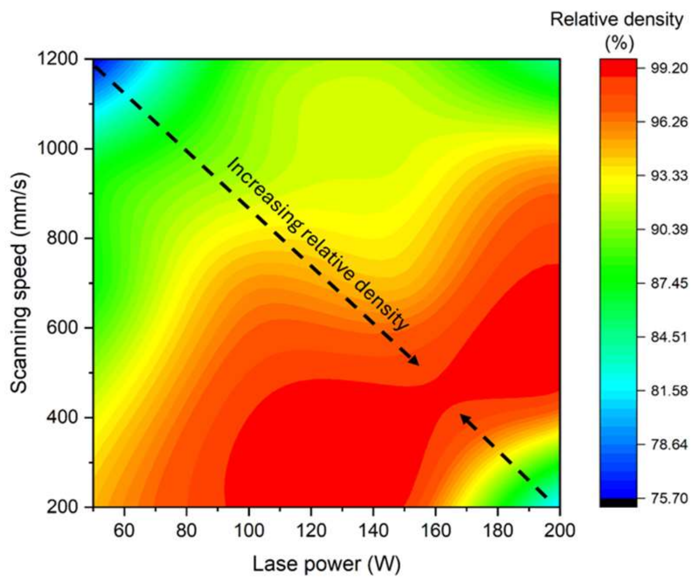

Relative density map of Inconel 718 solid block fabricated by varying different processing parameters.

- **Lattice Structures**
  - Open-cell porosity inversely related to energy input
  - Deviations from designed porosity at extreme settings

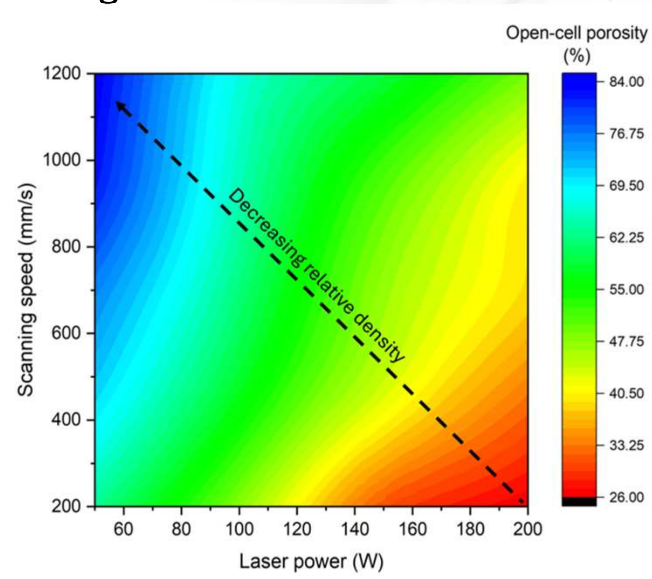

Open-cell porosity map of Inconel 718 lattice structures fabricated by varying different processing parameters.

Geometrical Characteristics

- **Open Pore Size and Strut Thickness**
  - Both decrease with increasing energy input
  - Side surfaces show more deviation than top surfaces
- **Dimensional Accuracy**
  - Closeness ratio introduced to quantify deviations
  - Optimal parameters minimize deviations from design

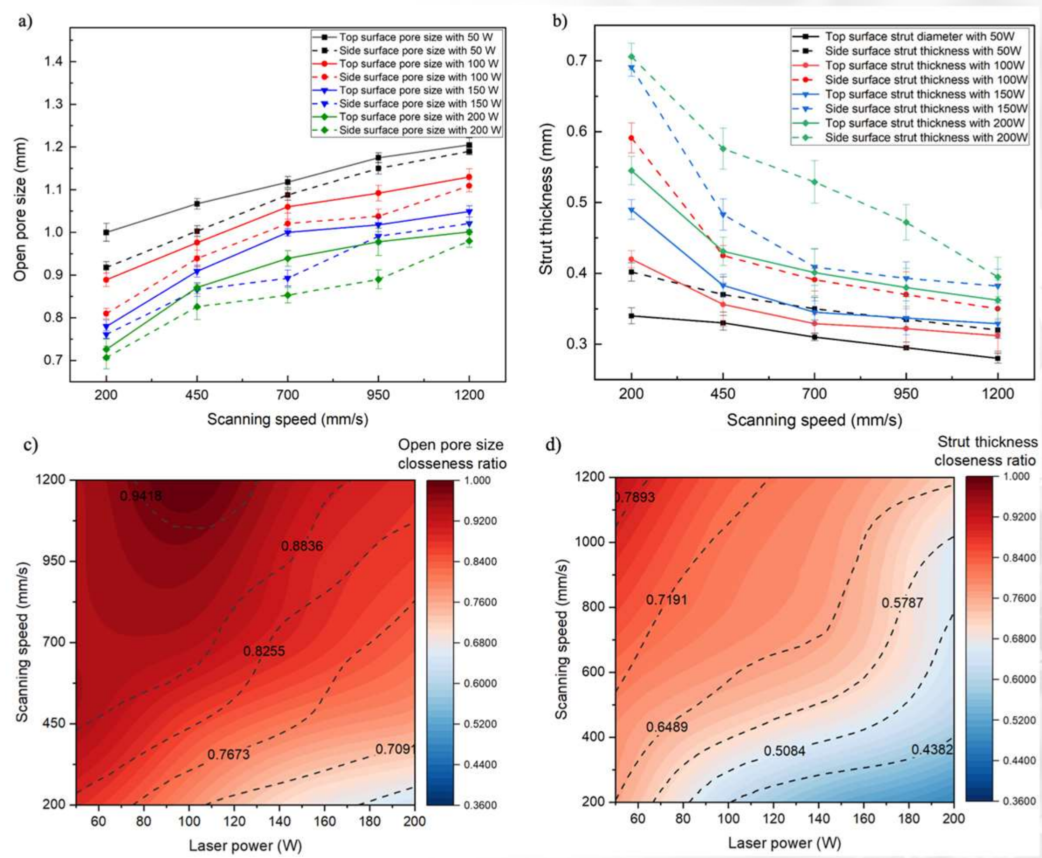

Variation of (a) open pore size and (b) strut thickness of the lattices as a function of laser power (W) and scanning speed (mm/s). Deviations of fabricated (c) open pore size, and (d) strut thickness from the intended design. The dashed lines indicate the values on the side surface.

ASME IMECE® 2024
International Mechanical Engineering Congress & Exposition®

Oregon State University
College of Engineering

Melt Pool Observations in Lattice Structures

1. **Low Energy Input (50 W, 1200 mm/s)**
   - **Melt Pool Depth**: ~36 µm
   - **Characteristics**:
     - High open-cell porosity
     - Larger pores, thinner struts
     - Minimal remelting preserves porosity
2. **Moderate Energy Input (100 W, 450 mm/s)**
   - **Melt Pool Depth**: ~95 µm
   - **Characteristics**:
     - Balanced fusion and porosity
     - Moderately thicker struts
     - Slightly reduced pore size
3. **High Energy Input (200 W, 200 mm/s)**
   - **Melt Pool Depth**: ~184 µm
   - **Characteristics**:
     - Low open-cell porosity
     - Thicker struts, smaller pores
     - Extensive remelting leads to denser structures

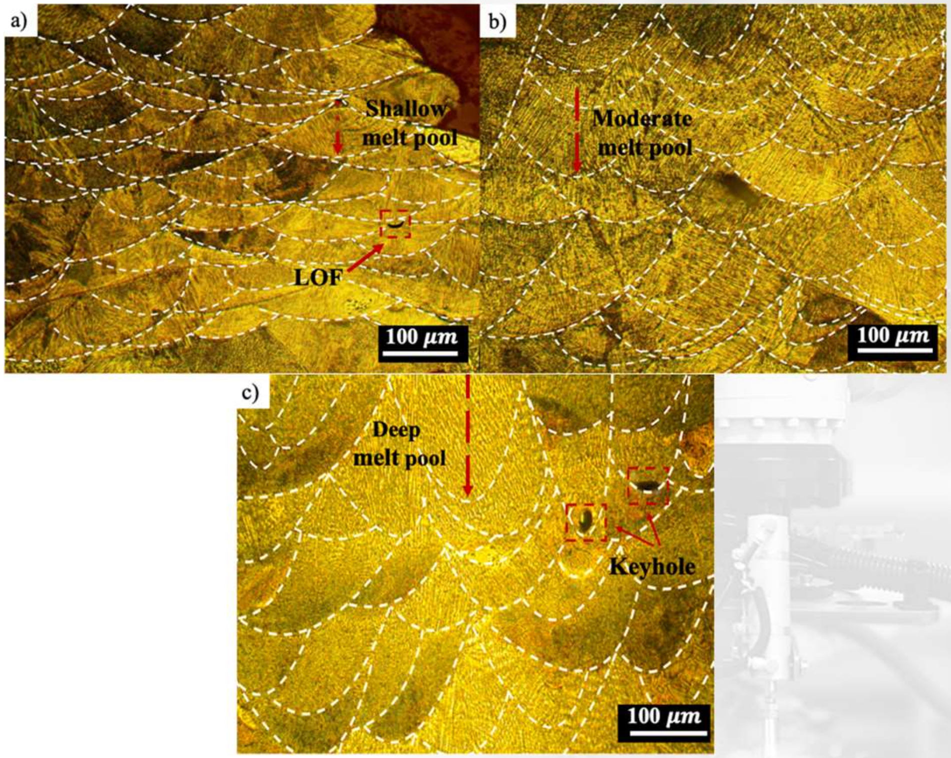

Melt pool geometry of lattices fabricated with (a) 50 W and 1200 mm/s, (b) 100 W and 450 mm/s, and (c) 200 W and 200 mm/s.

Surface Roughness Analysis

- **Top Surfaces**
  - Roughness decreases with increased laser power and decreased scanning speed

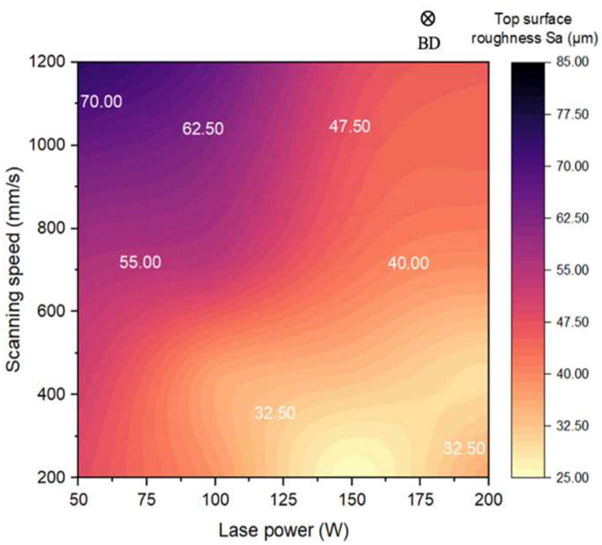

Figure 7. Areal surface roughness Sa of top surfaces of the lattices as a function of laser power (W) and scanning speed (mm/s).

- **Side Surfaces**
  - Generally higher roughness than top surfaces
  - Influenced by powder adhesion and staircase effect

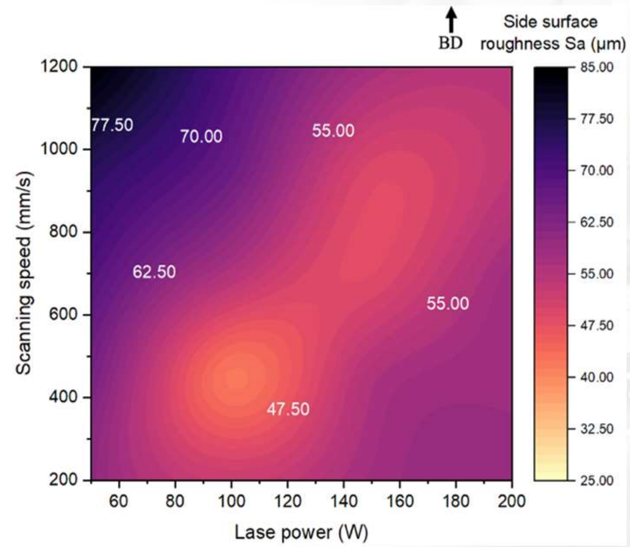

Areal surface roughness Sa of side surfaces of the lattices as a function of laser power (W) and scanning speed (mm/s).

Crystallographic Orientation via XRD Analysis

- **Observation**: Intensity of (002) peak increases with energy input
- **Lotgering Factor (L(001))**
  - Quantitative measure of (001) grain orientation
  - **Equation** [1,2,3]:

$$L(001) = \frac{A(00l) - B(00l)}{1 - B(00l)}$$

$$A(00l)\ and\ B(00l) = \frac{\sum Int(00l)}{\sum Int(hkl)}$$

- **Results**
  - L(001) increases with energy density
  - Indicates stronger (001) orientation at higher energy inputs

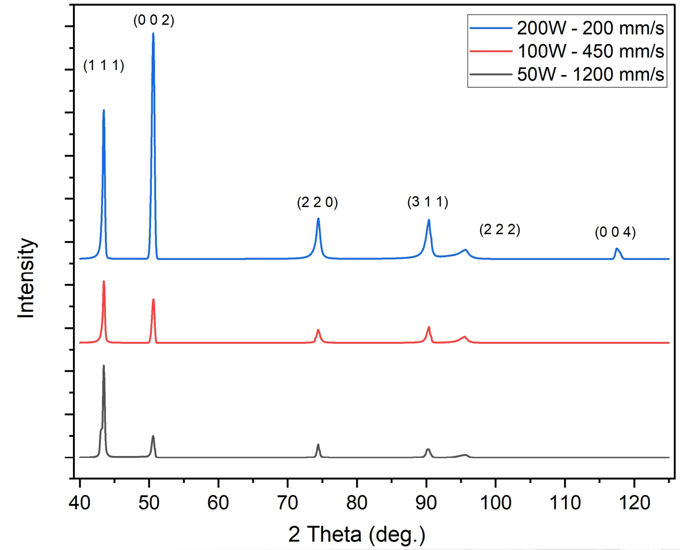

XRD patterns for 3 of the Inconel 718 fabricated lattices fabricated under different processing parameters.

	Energy density(J/mm2)	L factor (001)
50 W- 1200 mm/s	1.04	0.06
100 W- 450 mm/s	5.55	0.25
200 W- 200 mm/s	25	0.41

1.Sun, S.-H.; Hagihara, K.; Nakano, T. Effect of Scanning Strategy on Texture Formation in Ni-25 at.%Mo Alloys Fabricated by Selective Laser Melting. *Mater Des* **2018**, *140*, 307–316. https://doi.org/10.1016/j.matdes.2017.11.060.
2.Hagihara, K.; Nakano, T.; Suzuki, M.; Ishimoto, T.; Suyalatu; Sun, S.-H. Successful Additive Manufacturing of MoSi2 Including Crystallographic Texture and Shape Control. *J Alloys Compd* **2017**, *696*, 67–72. https://doi.org/10.1016/j.jallcom.2016.11.191.
3.Gokcekaya, O.; Hayashi, N.; Ishimoto, T.; Ueda, K.; Narushima, T.; Nakano, T. Crystallographic Orientation Control of Pure Chromium via Laser Powder Bed Fusion and Improved High Temperature Oxidation Resistance. *Addit Manuf* **2020**, *36*, 101624.

Oregon State University
College of Engineering

Mechanical Testing—Shear Tests

- **Sample Preparation and testing condition**
  - Cylindrical samples (ϕ 5 mm × 10 mm)
  - Shear load applied perpendicular to build direction with rate of 2 mm/min at room temperature

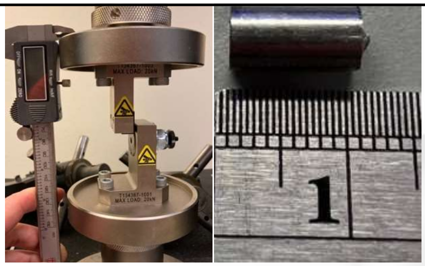

The shear fixture used in this study

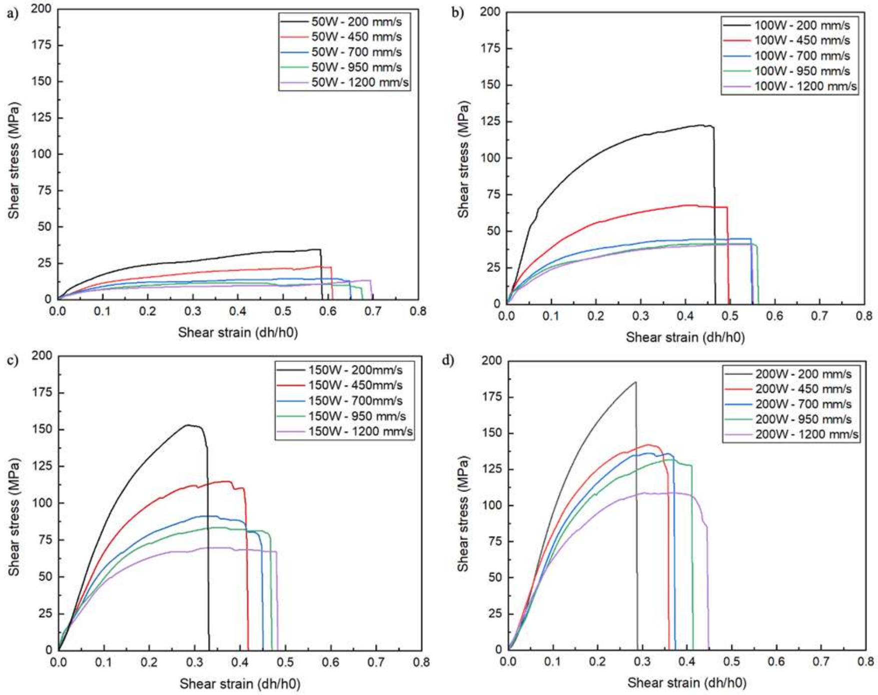

Shear stress vs. shear strain curve for fabricated lattices under (a) 50 W, (b) 100 W, (c) 150 W, and (d) 200 W.

Parameter set	Ultimate shear strength (Mpa)	Parameter set	Ultimate shear strength (Mpa)
50-200	34.4	150-200	153.2
50-450	22.6	150-450	114.9
50-700	14.4	150-700	91.1
50-950	13.1	150-950	83.3
50-1200	11.5	150-1200	69.7
100-200	122.5	200-200	185.5
100-450	67.9	200-450	142
100-700	44.9	200-700	136.1
100-950	41.5	200-950	131.6
100-1200	41	200-1200	108.8

Oregon State University College of Engineering

Fractography Analysis

- **Higher open cell porosity lattices:**
  - Ductile failure, gradual deformation
  - Visible dimples, rough fracture surfaces
- **Lower open cell porosity lattices:**
  - Brittle failure, abrupt collapse
  - Smooth, shiny surfaces, minimal deformation

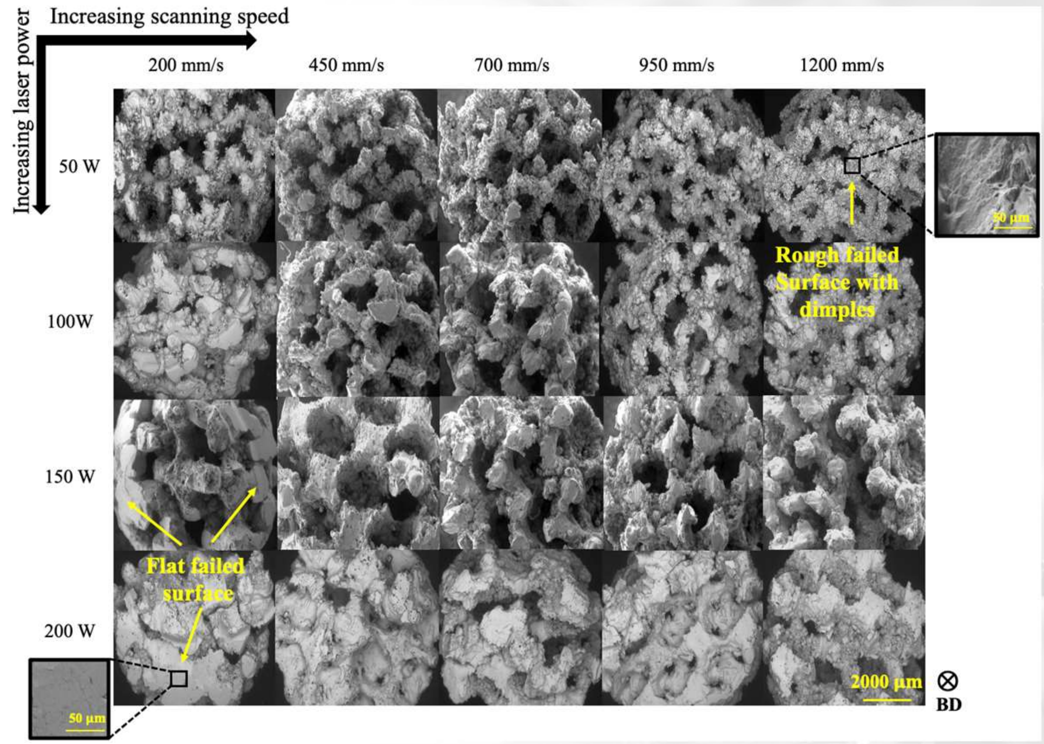

SEM micrographs of the fractured surface of the shear-tested samples fabricated under different processing parameters.

Limitations of Volumetric Energy Density (VED)

- Commonly used to predict micro/macrostructures in LPBF parts
- **Limitations of VED**
  - Does not account for material-specific thermal properties or melting enthalpy
  - Can lead to incomplete understanding of thermal dynamics
- **Illustrative Example**
  - **Lattice A**: 50 W, 200 mm/s (VED = 250 J/mm³), Open-cell porosity = 63%
  - **Lattice B**: 200 W, 950 mm/s (VED = 210 J/mm³), Open-cell porosity = 40%
  - Despite higher VED, Lattice A has higher porosity—**contradicts expectations**

$$\mathrm{VED} = \frac{P}{V.H.L}$$

P: Laser Power
V: Scanning Speed
H: Hatch Spacing
L: Layer Thickness

ASME IMECE® 2024 International Mechanical Engineering Congress & Exposition®

Oregon State University College of Engineering

Normalized Enthalpy—A Superior Metric

- Normalized Enthalpy Incorporates Material Properties [1]
- **Advantages Over VED**
  - **Better Correlation** with observed porosity changes
  - **Identifies Melt Pool Modes**:
    - **Low enthalpy (2-11)**: Lack of Fusion Mode
    - **Moderate enthalpy (11-33)**: Conduction Mode
    - **High enthalpy (33-50)**: Keyhole Mode

$$\overline{\Delta H} = \frac{\alpha P}{\rho (L_H + C\Delta T)\sqrt{DV\pi\omega^3}}$$

α: Absorptivity
ρ: Density
LH: Latent Heat of Fusion
C: Specific Heat Capacity
ΔT: Temperature Range
D: Thermal Diffusivity
V: Scanning Speed
ω: Laser Spot Size

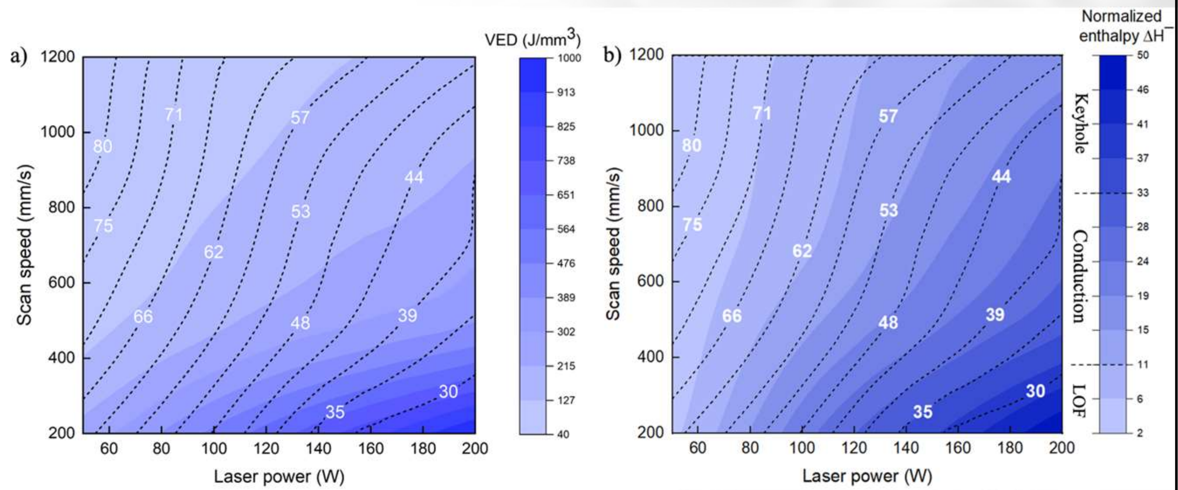

(a) VED (J/mm3), and (b) normalized enthalpy map with variation of processing parameters. The colored contour represents VED and normalized enthalpy while the dashed lines together with the white values represent the open-cell porosity of the fabricated lattices.

Property	units	Value	Ref.
Density	$\frac{Kg}{m^3}$	8190	[52]
Absorptivity	-	0.32-0.75	[53]
Latent heat of fusion	$\frac{J}{Kg}$	$2.19 \times 10e^5$	[54]
Solidus temperature	K	1528	[55]
Liquidus temperature	K	1610	[55]
Specific heat	$\frac{J}{Kg.K}$	0.42 - 0.63	[56]
Thermal diffusivity	$\frac{m^2}{S}$	$4.98 \times 10e^{-6}$	[56]
Laser spot size	m	$4 \times 10^{-6}e^{-6}$	

1- Ghasemi-Tabasi, H.; Jhabvala, J.; Boillat, E.; Ivas, T.; Drissi-Daoudi, R.; Logé, R. E. An Effective Rule for Translating Optimal Selective Laser Melting Processing Parameters from One Material to Another. *Addit Manuf* **2020**, *36*, 101496. https://doi.org/10.1016/j.addma.2020.101496.

ASME IMECE® 2024 International Mechanical Engineering Congress & Exposition®

Oregon State University College of Engineering

Acknowledgment

- This project is supported by the U.S. Department of Energy's Office of Energy Efficiency and Renewable Energy (EERE) under the Bioenergy Technologies Office under Award Number DEEE0009261and by Oregon State Lottery funds administered by the Oregon Business Development Department (award #: C2021177).

- The views expressed herein do not necessarily represent the views of the U.S. Department of Energy or the United States Government.

- We would like to thanks the OSU Electron Microscopy Center and Advanced Technology and Manufacturing Institute (ATAMI)

Oregon State University

ATAMI

MAGMA Metal Additive & Gradient Microstructure Alloys